Serum Stable and Low Hemolytic Temporin-SHa Peptide Analogs Disrupt Cell Membrane of Methicillin-Resistant Staphylococcus aureus (MRSA)

Rukesh Maharjan, Arif Iftikhar Khan, Muhammad Nadeem-Ul-Haque, Marc Maresca, M Iqbal Choudhary, Farzana Shaheen, Shabana U Simjee

Serum Stable and Low Hemolytic Temporin-SHa Peptide Analogs Disrupt Cell Membrane of Methicillin-Resistant *Staphylococcus aureus* (MRSA)

Rukesh Maharjan[1] · Arif Iftikhar Khan[1] · Muhammad Nadeem-ul-Haque[1] · Marc Maresca[2] · M. Iqbal Choudhary[1,3,4,5] · Farzana Shaheen[1,4] · Shabana U. Simjee[1,3]

Accepted: 28 December 2021

Abstract

Anti-microbial peptides (AMPs) have attracted major attention due to their potential bio-activities against some multidrug resistant pathogens. The present study evaluated the mechanism of actions of highly potent AMP temporin-SHa analogs, i.e., [G4a]-SHa, [G7a]-SHa, and [G10a]-SHa, against methicillin-resistant *Staphylococcus aureus* (MRSA) NCTC (13277) with minimum inhibitory concentrations (MICs) of 14.35, 7.16, and 3.58 µM, respectively. These analogs exhibited significant anti-MRSA activity at physiological salt concentration, 30% fetal bovine serum, and 30% human serum. [G4a]-SHa and [G7a]-SHa were non-hemolytic and non-cytotoxic to normal mouse fibroblast 3T3 cell and human Caco-2 cell line. Atomic force microscopy revealed that these analogs have profound effect on the morphological changes in MRSA surface with significant leakage of cell cytoplasmic content. Propidium iodide uptake kinetic assay and (bis-(1,3-dibutylbarbituric acid) trimethine oxonol) $DiBAC_4(3)$ membrane depolarization assay demonstrated that these analogs display a membrane disrupting property, characterized by elevation of plasma membrane permeability and rapid transmembrane potential depolarization. [G10a]-SHa showed a significant anti-biofilm activity against biofilm forming *S. aureus* (ATCC 6538). Acute *in vivo* toxicity studies revealed that [G10a]-SHa possesses some toxic effect at 100-mg/kg dose. While [G4a]-SHa at 100 mg/kg, i.p. has no toxic effect even after 48 h, [G7a]-SHa also did not show any toxic effect at the dose of 100 mg/kg, i.p. during 24-h observation of animals. In conclusion, [G4a]-SHa, [G7a]-SHa, and [G10a]-SHa show improved activity against MRSA and stability compared to SHa peptide. Although highly potent, [G10a]-SHa, due to its hemolytic activity, might be more suitable for topical application, whereas [G4a]-SHa and [G7a]-SHa have potential to be used for systemic application.

Keywords AMPs · Bacterial cell membrane · D-alanine · MRSA · Temporin-SHa · MDR *Staphylococcus aureus*

✉ Farzana Shaheen
afnan.iccs@gmail.com; farzana.shaheen@iccs.edu

✉ Shabana U. Simjee
shabana.simjee@iccs.edu

[1] International Center for Chemical and Biological Sciences, H. E. J. Research Institute of Chemistry, University of Karachi, Karachi 75270, Pakistan

[2] Aix Marseille Univ, CNRS, Centrale Marseille, iSm2, 13397 Marseille, France

[3] Dr. Panjwani Center for Molecular Medicine and Drug Research, International Center for Chemical and Biological Sciences, University of Karachi, Karachi 75270, Pakistan

[4] Third World Center for Science and Technology, International Center for Chemical and Biological Sciences, University of Karachi, Karachi 75270, Pakistan

[5] Department of Biochemistry, Faculty of Science, King Abdulaziz University, Jeddah 21589, Saudi Arabia

Introduction

The prevalence of methicillin-resistant *Staphylococcus aureus* (MRSA) has become a global problem because of its associated notorious hospital and community infections [1]. Vancomycin is a drug of choice for treating MRSA infections, but in 1997 vancomycin intermediate *Staphylococcus aureus* (VISA) was reported in Japan [2], causing a widespread alarm. Thus, the crisis of anti-microbial resistance has kept classical antibiotics under intense scrutiny. To overcome this, several investigations have been carried out over the last few decades to develop alternative treatments. Among the several classes of anti-bacterial agents, anti-microbial peptides (AMPs) have received special attention because of their broad-spectrum anti-microbial activity. AMPs play an important role in host defense in eukaryotes,

and are considered as a possible alternative way to combat antibiotic-resistant bacterial strains.

Among the 13 families of AMPs isolated from the skins of frogs of the Ranidae family [3, 4], short peptide like temporins received special attention as potential drug candidate because of low manufacturing cost [5]. Temporins are *C*-terminally amidated small-sized peptides comprising of essential, direct, profoundly hydrophobic AMPs containing 10–14 amino acids with a net positive charge (0 to + 3). These AMPs adopt an amphipathic α-helical structure in membrane mimetic environments or in apolar media [6, 7]. The amphipathic α-helical structure of different temporins enables them to interact with different microbial, and mammalian cell membranes, through different mechanisms such as toroidal pores, carpet-like, barrel-stave, or channel aggregates [6, 8–10].

Temporin-SHa of the temporin family is a single lysine basic residue containing AMP, isolated from the skin of the North African frog *Pelophylax saharica* [11]. It is reported to have a broad spectrum anti-bacterial, anti-fungal, and anti-leishmanial activities, being highly hemolytic and cytotoxic in nature. Ladram et al. (2017) [12] and Raja et al. (2017) [13] studied [K3-SHa] analog, which showed more potent anti-microbial activity than the parent peptide (SHa). Recent study has shown that gold surfaces coated with SHa, and its lysine substituted analogs, retained anti-bacterial and anti-adhesive properties against Gram-positive bacteria *Listeria ivanovii* [14]. This made them possible candidates as anti-microbial coating agents [15]. Recently, SHa anti-bacterial activity against *Helicobacter pylori* [16], *Legionella pneumophila* [17], and anti-cancer activity against breast, cervical, and lung cancers [18] have been published. Shah et al. have shown a higher efficacy of temporin-LK1 analog by substituting glycine with D-alanine [19].

In the present study, the peptide analogs of temporin-SHa were synthesized by replacing glycine with single D-alanine at three different positions (4, 7, and 10). This was based on the hypothesis to make them more serum stable and less cytotoxic. These analogs were evaluated first time for anti-MRSA activity, along with cytotoxicity, hemolysis, and salt and serum sensitivity, as well as their mechanistic studies by using different techniques, and acute *in vivo* toxicity profile.

Methodology

Synthesis of D-Alanine Substituted Analogs of Temporin-SHa

Peptides were synthesized manually by following Fmoc solid phase peptide synthesis method as described by Shaheen et al. [18]. Further purification of peptides was carried out on LC-908 W recycling preparative-HPLC (Japan Analytical Industry, Tokyo, Japan) with a column of ODS-MAT80 (C18). ^{1}H- and ^{13}C-NMR spectra of these purified peptides were recorded at room temperature on Bruker nuclear magnetic resonance (NMR) spectrometers (Bruker, Zürich, Switzerland) with operating frequency at 600 MHz and 125 MHz, respectively [16].

Mass Spectrometric Analysis of Peptides

Matrix-assisted laser desorption/ionization–time of flight (MALDI-TOF) analysis of the peptides was carried out on Ultraflex III TOF/TOF (Bruker Daltonics, Germany) mass spectrometer [16, 18]. Electrospray ionization quadrupole time-of-flight (ESI-QTOF-MS) mass spectra were carried out on Q-STAR XL mass spectrometer (Applied Biosystems, USA).

Determination of Minimum Inhibitory Concentration (MIC) by Using AlamarBlue Assay, Minimum Bactericidal Concentration (MBC), and Salt and Serum Sensitivity

A single colony of *Staphylococcus aureus* (NCTC 13,277) was inoculated in Mueller Hinton Broth (MHB) (Oxoid, UK), and incubated overnight at 37 °C [20]. Stock solutions of different peptides (10 mM) prepared in DMSO were then two-fold diluted in MHB broth ranging between 100 and 1.5 µM. Bacterial suspension, adjusted to 0.5 McFarland Turbidity Index, was then diluted to make up the final volume of 200 µL to achieve $0.5–1.0 \times 10^{6}$ CFU/mL. Plates were then incubated for 18–20 h at 37 °C. MIC value was assigned to the lowest concentration of the test peptides which did not support visible growth. The same procedure was followed for these peptides at different physiological salt concentrations of NaCl, $MgCl_2$, $CaCl_2$, 30% fetal bovine serum, 30% human serum, and 10% human blood to check salt sensitivity, serum, and blood effect, respectively. For quantitative analysis, 20 µL of 0.02% resazurin sodium salt dye (Sigma-Aldrich, USA) was added in all wells, and incubated at 37 °C in shaking incubator at 80 rpm for 2 h. The bacterial growth was indicated by change in the color of dye from blue to reddish pink. Absorbance was read at 570 and 600 nm in Multiskan GO spectrophotometer (Thermo Scientific, USA). The % difference in reduction of dye due to bacterial growth was calculated using the mentioned formula [21].

$$\text{Percent difference in reduction} = \frac{(\varepsilon\text{OX})\lambda 2A\lambda 1 - (\varepsilon\text{OX})\lambda 1A\lambda 2 \text{ of test agent dilution}}{(\varepsilon\text{OX})\lambda 2A^{\circ}\lambda 1 - (\varepsilon\text{OX})\lambda 1A^{\circ}\lambda 2 \text{ of untreated positive growth control}} \times 100$$

where ε_{OX} is the molar extinction coefficient (80,586 and 117,216 M^{-1} cm^{-1}) of AlamarBlue® at two different wavelengths λ_1 (570 nm) and λ_2 (600 nm), respectively, and A and A° show the absorbance of test and positive growth control (media and bacterial cells) wells.

Subsequently, % inhibition of bacteria due to compound was calculated by subtracting % reduction from 100. For MBC, 5-µL aliquots were taken from the treated wells of different concentrations of test peptides, and added to a sterile petri dish. Melted tryptic soya agar (TSA) was added to these dishes, and incubated for 18–22 h at 37 °C. The bacterial growth was observed next day. Absence of bacterial colony with minimum concentration value was assigned MBC. All experiments were carried out in triplicates.

Hemolytic Assay

Fresh whole blood (3 mL) was obtained from a healthy volunteer in compliance with Independent Ethics Committee of International Center for Chemical and Biological Sciences (ICCBS) (Approval number ICCBS/IEC-047-HB-2019/Protocol/1.0). The blood was centrifuged and the cell pellet was washed thrice with PBS, and diluted to attain approximately 4% concentration of initial blood cells [22]. Peptide analog solutions (100 µL) at different concentrations (360, 180, 90, 45, 22.5, 11.25, 5.625, and 2.812 µM) were prepared in 2% DMSO, and mixed with 100 µL of RBC suspension. After 1 h incubation at 37 °C, the plate was centrifuged at 2500 × rpm for 10 min to separate non-hemolyzed red blood cells. The resulting supernatants (100 µL each) were transferred to a new 96-well plate, and the hemoglobin release was measured at 576 nm, using a spectrophotometer (MultiSkan Go, Thermo Scientific). Each assay was performed in triplicate, and the data were expressed as mean ± S.D.

$$\%\ \text{Hemolysis} = \frac{(\text{O.D. 576 nm of the treated sample} - \text{O.D. 576 nm of the negative control})}{(\text{O.D. 576 nm of the positive control} - \text{O.D.576 nm of the negative control})} \times 100$$

Cytotoxicity Assay Against Mouse Fibroblast NIH/3T3 (ATCC® CRL-1658™) and Human Colon Cancer Caco-2 (ATCC® HTB37™) Cell Lines

NIH/3T3 (ATCC® CRL-1658™) and Caco-2 (ATCC® HTB37™) cell lines were obtained from the cell culture bank of the Dr. Panjwani Center for Molecular Medicine and Drug Research, ICCBS, University of Karachi. These cell lines were cultured in Dulbecco's Modified Eagle Medium (DMEM) (Gibco, ThermoFisher Scientific, UK) supplemented with 10% fetal bovine serum and incubated in 5% CO_2 incubator at 37 °C. The cells were seeded at a density of 5000 cells/well of 96-well plate. Next day, 200 µL of fresh complete medium containing different concentrations of test peptides was added. After 24-h incubation, old medium was removed, and 200 µL of fresh medium containing thiazolyl blue tetrazolium bromide (MTT) (0.5 mg/mL) dye (Sigma-Aldrich, USA) was added [23]. After 3-h incubation, solution was discarded, and 100 µL of DMSO was added to solubilize the formazan crystals. After 10 min, absorbance was recorded at 540 nm using a microplate reader (Multiskan™ GO, Thermo Scientific, USA). The extent of MTT reduction to formazan crystals within the cells and the percent inhibition were calculated by using the formula given below. IC_{50} values were also calculated by using Microsoft Excel.

$$\%\ \text{Inhibition} = 100 - \frac{(\text{O.D. of test compound} - \text{O.D. of media control})}{(\text{O.D. of untreated control} - \text{O.D. of media control})} \times 100$$

Atomic Force Microscopy Study

Exponentially growing *S. aureus* cells, adjusted to 2–3 × 10^7 CFU/mL were treated with half and double MIC of

Table 1 Amino acid sequence of temporin-SHa and its analogs

Peptide code and substitution	Sequence[a]	Chemical formula	Calculated mass[b]	Observed mass[c]
SHa	F[1]-L[2]-S[3]-G[4]-I[5]-V[6]-G[7]-M[8]-L[9]-G[10]-K[11]-L[12]-F[13]-NH2	$C_{67}H_{109}N_{15}NaO_{14}S$	1402.7891	$[M+Na]^+$ = 1402.7896
[G10a]-SHa	F[1]-L[2]-S[3]-G[4]-I[5]-V[6]-G[7]-M[8]-L[9]-**a[10]**-K[11]-L[12]-F[13]-NH2	$C_{68}H_{112}N_{15}O_{14}S$	1394.823	$[M+H]^+$ = 1394.822
[G4a]-SHa	F[1]-L[2]-S[3]-**a[4]**-I[5]-V[6]-G[7]-M[8]-L[9]-G[10]-K[11]-L[12]-F[13]-NH2	$C_{68}H_{111}N_{15}NaO_{14}S$	1416.8053	$[M+Na]^+$ = 1416.8048
[G7a]-SHa	F[1]-L[2]-S[3]-G[4]-I[5]-V[6]-**a[7]**-M[8]-L[9]-G[10]-K[11]-L[12]-F[13]-NH2	$C_{68}H_{111}N_{15}NaO_{14}S$	1416.8053	$[M+Na]^+$ = 1416.8084

a D-alanine, *F* phenylalanine, *G* glycine, *I* isoleucine, *K* lysine, *L* leucine, *M* methionine, *S* serine, and *V* valine

[a]The substituted D-alanine residue is indicated in small bold letter (**a**) in the sequence

[b]Calculated mass

[c]Observed mass using HR-MALDI

each active peptide [24] and incubated for 30 min at 37 °C. Cells were then centrifuged and washed with sterile analytical grade water to remove peptides. Control and treated bacterial cells in a volume of 10 µL were applied on a silicon wafer, which was pretreated with (0.01%) poly-L-lysine (Sigma-Aldrich, USA), and allowed to dry before imaging. Changes in bacterial morphology due to peptide effect were monitored by atomic force microscopy (AFM) (Agilent Technologies 5500, USA) in tapping mode, with silicon nitride high-resonance frequency cantilever (Nominal

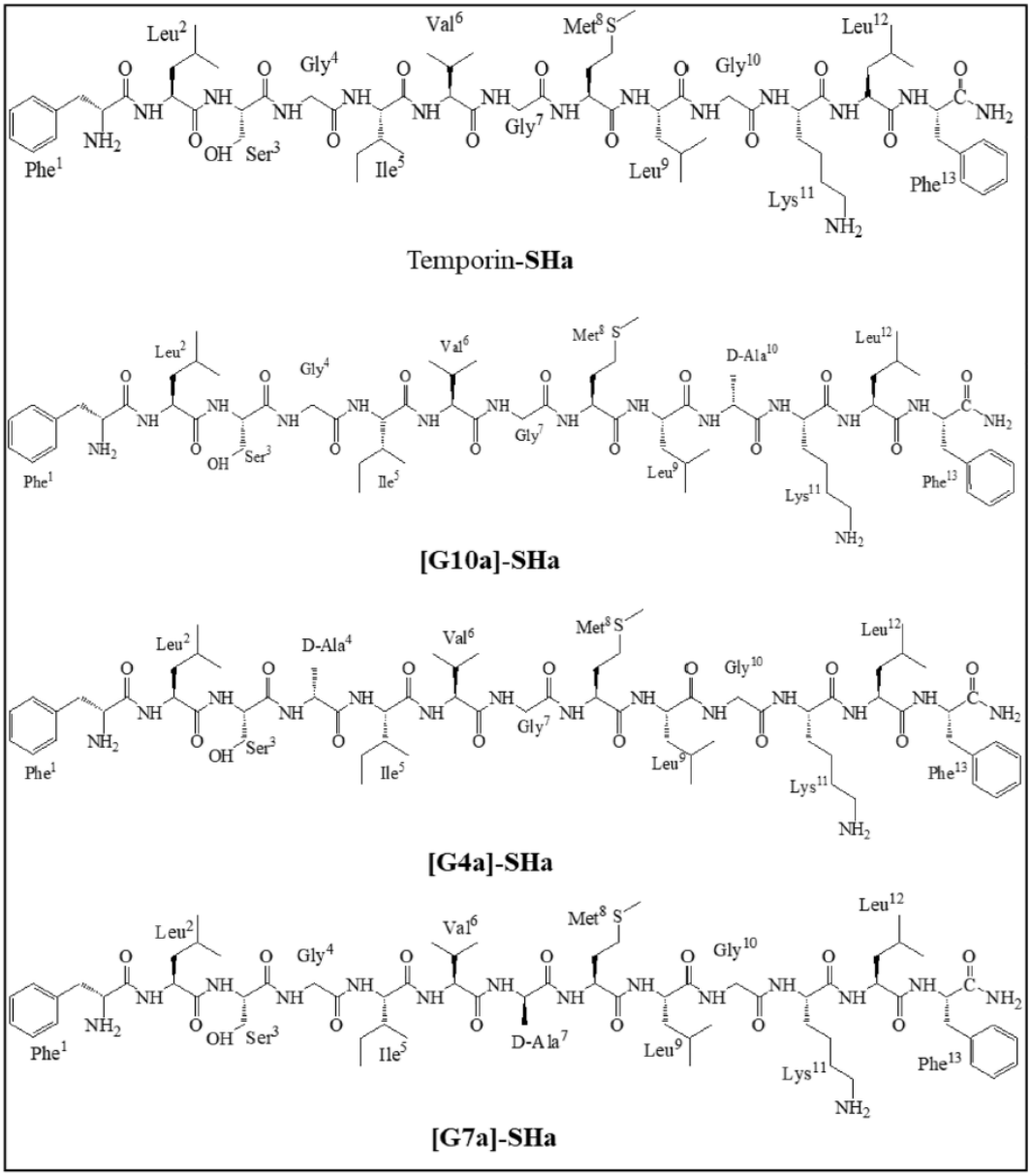

Fig. 1 Chemical structures of temporin-SHa, [G10a]-SHa, [G4a]-SHa, and [G7a]-SHa

resonant frequency = 330 kHz). Images were analyzed in PicoView 1.2 imaging software.

Cell Membrane Potential and Cell Membrane Permeability Assay

The protocol of Clementi et al. [25] was followed. A stock solution of propidium iodide (PI) dye (1 mg/mL in double-distilled H_2O) (Sigma-Aldrich, USA) and (bis-(1,3-dibutylbarbituric acid) trimethine oxonol) $DiBAC_4(3)$ dye (50 µM in DMSO) (Sigma-Aldrich, USA) was prepared, and final working concentrations of 10 µg/mL and 250 nM, respectively, were used in cell suspension. The exponential growth phase bacterial cells were washed with PBS at a concentration of 10^8 CFU/mL, and then were supplemented with 1 M sterile glucose. Different concentrations of active peptide were placed in cell suspension in triplicate. After proper mixing, 200 µL of this cell suspension was placed into each well of a white polystyrene 96-well plate. The plate was placed in a 37 °C fluorescence detection plate reader (SpectraMax M2, USA), and appropriate filter was placed for $DiBAC_4(3)$ and PI dye (excitation/emission — 490/516 nm and 535/617 nm, respectively). To check cell membrane potential, $DiBAC_4(3)$ fluorescence was monitored for 30 min at intervals of 5 min. To assess cell membrane permeability, PI fluorescence was taken for 2 h at 15-min intervals. The graph of fluorescence over time was plotted.

Minimum Biofilm Inhibitory Concentration (MBIC) Using Crystal Violet Assay

Mid-log phase strong biofilm forming *S. aureus* (ATCC 6538) in brain heart infusion broth, supplemented with 0.25% glucose at $0.5–1.0 \times 10^6$ CFU/mL, was treated with SHa analogs in 96-well plate and incubated overnight at 37 °C [26]. Next day, plate was washed, dried, then stained with 0.1% crystal violet dye, and washed again. After drying, images of these wells were taken in microscope and then 200 µL of 30% acetic acid was added into each well, and the absorbance was measured at 595 nm by using a spectrophotometer (Thermo Scientific, USA). Percent inhibition was calculated as

$$\% \text{ Inhibition} = 100 - \frac{(\text{O.D. of test compound} - \text{O.D. of media control})}{(\text{O.D. of untreated control} - \text{O.D. of media control})} \times 100$$

Acute *In Vivo* Toxicity Model

In vivo experiment was carried out with the approved animal study protocol number (#2019–013) on September 30, 2019 from the Institutional Animal Care And Committee (IACAC), ICCBS, University of Karachi. Each group contained healthy pathogen free 4 female BALB/c mice weighing 21–25 g. Three different doses (25, 50, and 100 mg/kg) of each peptide were given by intra-peritoneal administration. The oral administration of [G7a]-SHa at doses of 25, 50, and 100 mg/kg was carried out to check its toxic effect on GIT. After administration of peptides, the animals were kept under observation for 48 h. Animals were closely monitored for any sign of toxicity. The number of dead and live animals for each dose was noted, and LD_{50} dose was calculated by using Up and Down method Botham [27].

Statistical Analysis

The data was statistically analyzed using GraphPad Prism 5.0 software. In propidium iodide and $DiBAC_4(3)$ dye uptake assay, two-way analysis of variance (ANOVA) at the significance level of $^*P < 0.05$ was used. In the remaining assays, treated groups were compared with untreated control and one-way analysis of variance (ANOVA) at the significance level of $^*P < 0.05$ with Dunnett post-test was applied.

Results

Synthesis of D-Alanine Substituted Temporin-SHa Analogs

Temporin SHa analogs, [G10a]-SHa, [G4a]-SHa, and [G7a]-SHa, were synthesized by substituting the glycine residue at positions 10, 4, and 7, respectively, with D-alanine, by using Fmoc peptide synthesis protocol (Table 1). The chemical structures of SHa, [G10a]-SHa, [G4a]-SHa, and [G7a]-SHa, are presented in Fig. 1.

Table 2 Susceptibility tests (MIC and MBC) of SHa and its analogs against MDR *S. aureus* (NCTC 13,277) by employing AlamarBlue® assay and their percentage inhibition (mean ± SD)

Compounds	MIC (µM)	MBC (µM)				% inhibition at 14.34 µM (mean ± SD)
		MHB	30% FBS	30% human serum	10% human blood	
SHa	3.62	29	159	> 220	> 220	90.198 ± 0.413
[G10a]-SHa	3.58	16	36	58	> 72	90.213 ± 0.253
[G4a]-SHa	14.34	57.35	143.38	143.38	186	83.243 ± 2.124
[G7a]-SHa	7.16	35.84	143.38	180	186	85.125 ± 1.254

Table 3 Susceptibility test (μM) of SHa and its analogs against MDR *S. aureus* (NCTC 13,277) at different physiological salt concentrations

Serial no	Peptides	NaCl (mM)			$MgCl_2$ (mM)			$CaCl_2$ (mM)		
		50	150	300	1	3	5	1	3	5
1	[G10a]-SHa	7.16	7.16	7.16	7.16	7.16	7.16	7.16	7.16	7.16
2	[G4a]-SHa	14.34	14.34	14.34	14.34	14.34	14.34	14.34	14.34	14.34
3	[G7a]-SHa	7.16	7.16	7.16	7.16	7.16	7.16	7.16	7.16	7.16

MIC, MBC, AlamarBlue Assay, Salt and Serum Sensitivity Assays

Anti-MRSA activity of SHa and its three analogs were tested against MRSA (NCTC 13,277), and cell viability was determined by using AlamarBlue assay. The MIC, MBC, and % inhibition at 14.34 μM of tested peptides is shown in Table 2. Peptide analogs [G4a]-SHa, [G7a]-SHa, and [G10a]-SHa showed better anti-MRSA activity with lower MIC values (14.34, 7.16, and 3.58 μM, respectively). Comparing the MIC and MBC values, [G10a]-SHa was found to be the most potent peptide, followed by [G7a]-SHa and [G4a]-SHa. All these analogs showed a good anti-bacterial activity even at high physiological salt and serum concentrations (300 mM NaCl, 5 mM $MgCl_2$, 5 mM $CaCl_2$, 30% fetal bovine serum, 30% human serum, and 10% human blood) (Tables 2 and 3). Analog [G10a]-SHa showed the most stability in all physiological salt and serum sensitivity assays, followed by [G4a]-SHa and [G7a]-SHa. The parent peptide was unstable in serum and decomposed due to which bacteria grew even at very high concentrations.

Cytotoxicity and Hemolytic Assays

Only peptide analogs [G10a-SHa] showed toxicity against RBCs with HB_{50} of 22.5 μM, and IC_{50} of 18 ± 1, and 55 ± 3 μM against NIH 3T3 and Caco-2 cell lines, respectively. Whereas, [G4a]-SHa and [G7a]-SHa were found to be non-cytotoxic to tested cells and less hemolytic in nature as compared to the parent peptide (Tables 4 and 5).

Table 4 Cytotoxicity (IC_{50}) of SHa and its analogs against NIH 3T3 and Caco-2 cell lines

Name of peptides	NIH 3T3 cell line IC_{50} value (μM)	Caco-2 ATCC HTB37 IC_{50} value (μM)
SHa	73.30 ± 5	> 100
[G10a]-SHa	18 ± 1	55 ± 3
[G4a]-SHa	> 100	> 100
[G7a]-SHa	> 100	> 100

The cytotoxicity and hemolytic assay results showed that D-alanine substitution at 4 and 7 positions of the parent peptide remarkably decreased the cytotoxic and hemolytic nature of [G4a]-SHa and [G7a]-SHa analogs, making them a suitable candidate for further study. [G10a]-SHa was proven to be highly active, but due to its hemolytic nature, it may be suitable only for topical applications.

Atomic Force Microscopy

Control cells displayed a smooth, compact, regular, and non-capsulated surface with cocci arranged in clusters. Structural integrity was well maintained with no visible pores, grooves, or rupture in the cell surfaces (Fig. 2a, b). Cells treated with half and double MIC of SHa and [G10a]-SHa were found to be swollen, rough with distinct irregular lines of disruption on the cell surface. Structural integrity was highly disturbed in double MIC-treated cells with no clear demarcation between the cells (Figs. 2c, d and 3a, b) respectively. In comparison to SHa, [G10a]-SHa-treated cells showed a higher degree of alterations in the structural integrity with higher cytoplasmic leakage. Cells treated with half and double MIC of [G4a]-SHa and [G7a]-SHa were also found to be rough with irregular and corrugated surfaces (Fig. 3c, d, e, f), respectively. Lines of rupture could be seen in many

Table 5 Percentage hemolysis assay of SHa analogs at different concentrations

Concentration (μM)	% hemolysis (mean ± SD)		
	[G10a]-SHa	[G4a]-SHa	[G7a]-SHa
2.812	< 1	< 1	< 1
5.625	1 ± 0.63	< 1	< 1
11.25	7 ± 0.56	< 1	1.8 ± 0.9
22.5	**52.74 ± 5.94**	2.88 ± 1.24	2 ± 0.94
45	55.07 ± 5.23	18.18 ± 7.65	7.49 ± 1.20
90	58.93 ± 6.02	**42.93 ± 4.75**	**44.69 ± 3.73**
180	61.64 ± 13.83	47.60 ± 7.88	57.01 ± 8.50
360	64.71 ± 11.34	51.15 ± 10.41	58.97 ± 5.51
Triton-X 100 (0.5%) Positive control	100		
DMSO (2%)	< 1		
PBS negative control	< 1		
Hb_{50} of SHa is 25 μM [6]			

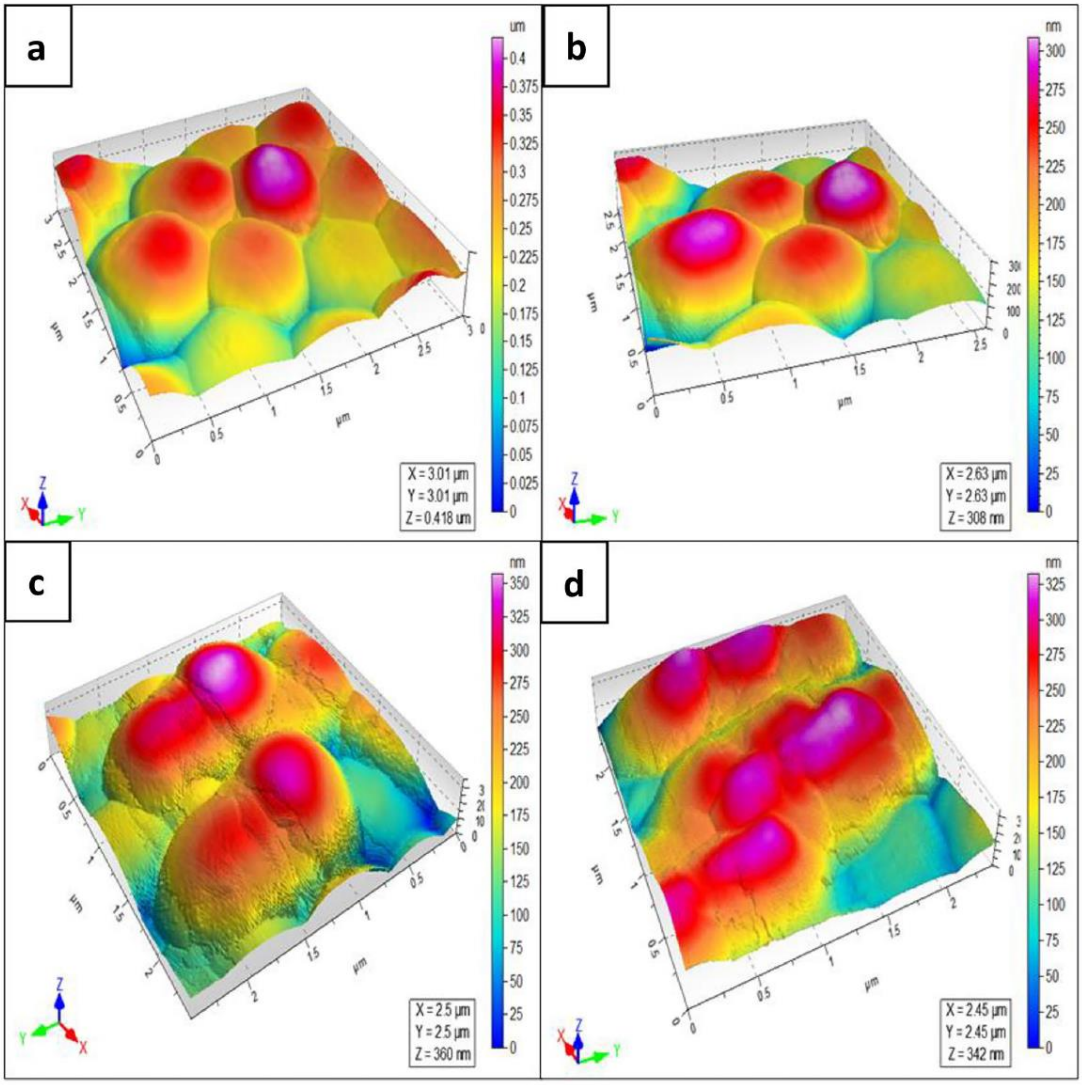

Fig. 2 Morphological evaluation of untreated and SHa-treated *S. aureus* (NCTC 13,277) by using atomic force microscopy. **a** and **b** Untreated control and **c** and **d** SHa-treated cells at half and double MIC, respectively

cells with alterations in the structural integrity, but with less leakage of cytoplasmic content, as compared to [G10a]-SHa.

Propidium Iodide (PI) Uptake Kinetic Assay

The relative fluorescence unit (rfu) of untreated *S. aureus* increased slightly due to the presence of small number of dead permeable cells. Cells treated with vancomycin and gentamycin showed a slight but non-significant increase in rfu values, as compared to untreated control cells (Fig. 4a). PI fluorescence intensity of cells treated with [G10a]-SHa (3.5, 7, 14, and 28 µM), [G4a]-SHa (14, 21, and 28 µM), and [G7a]-SHa (7, 14, and 28 µM) increased significantly ($P < 0.001$), as compared to the untreated control (Figs. 4b and 5a, b), respectively. [G10a]-SHa-treated cells at a dose higher than 14 µM showed higher fluorescence above 1400 rfu, indicating its strong cell membrane rupturing ability.

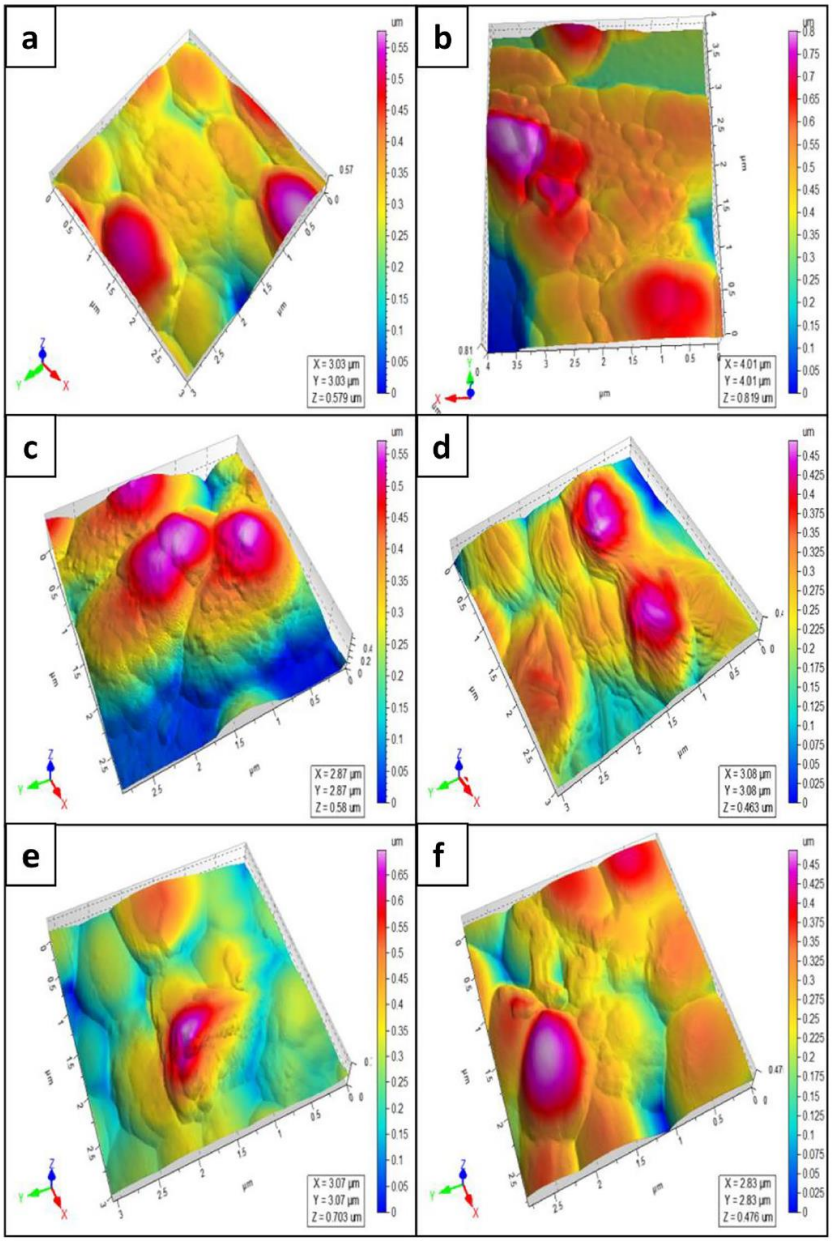

Fig. 3 Morphological evaluation of [G10a]-SHa-, [G4a]-SHa-, and [G7a]-SHa-treated *S. aureus* (NCTC 13,277) by using atomic force microscopy. **a** and **b** [G10a]-SHa-treated cells at half and double MIC, respectively; **c** and **d** [G4a]-SHa-treated cells at half and double MIC, respectively; and **e** and **f** [G7a]-SHa-treated cells at half and double MIC, respectively

$DiBAC_4(3)$ Membrane Depolarization Assay

MRSA cells treated with Triton-X showed significant increase ($P < 0.001$) in fluorescence, whereas gentamycin- and vancomycin-treated cells showed non-significant difference as compared to untreated control (Fig. 6a). MRSA cells treated with SHa (Fig. 6b) and [G10a]-SHa (Fig. 7a) at 14-, 28-, and 42-µM doses demonstrated significant increase ($P < 0.001$) in fluorescence at all-time intervals. The maximum fluorescence of SHa and [G10a]-SHa at 42 µM was 20,014 and 25,737 rfu, respectively. MRSA cells treated with [G4a]-SHa (Fig. 7b) and [G7a]-SHa (Fig. 7c) at 14, 28, and 42 µM showed significant increase in fluorescence ($P < 0.001$) at 5 min after treatment;

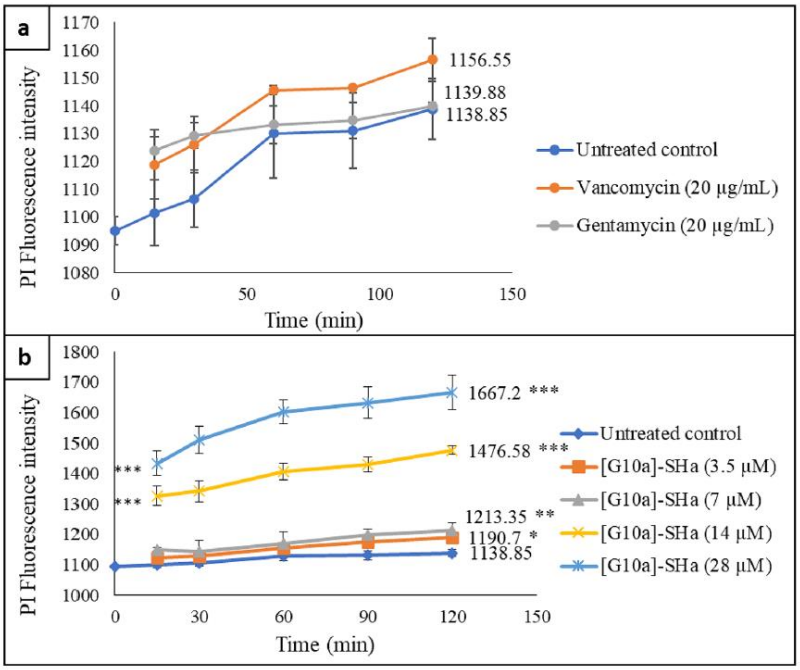

Fig. 4 Propidium iodide (PI) uptake kinetic assay of untreated and [G10]-SHa-treated *S. aureus* (NCTC 13,277) cells. **a** Untreated control and standard drug-treated cells and **b** [G10a]-SHa-treated cell, where $*P<0.05$, $**P<0.01$, and $***P<0.001$ as compared to untreated *S. aureus*

thereafter, fluorescence gradually decreased. However, at 30 min, this decrease in fluorescence was still significantly higher ($P<0.001$) than the untreated control. These results showed the membrane depolarizing effect of these peptides which consequently increased the membrane permeability, and compromised its membrane integrity.

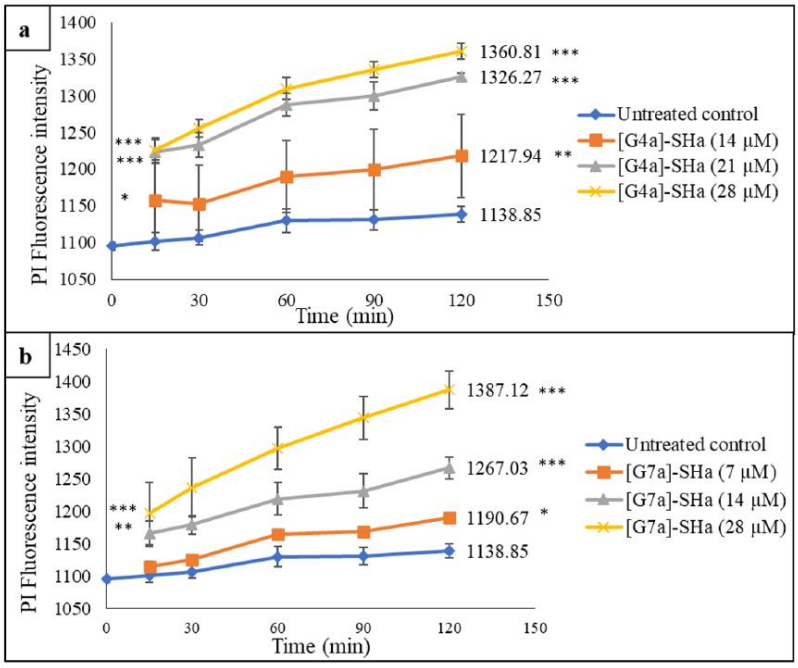

Fig. 5 Propidium iodide (PI) uptake kinetic assay of *S. aureus* (NCTC 13277) cells treated with [G4a]-SHa and [G7a]-SHa. **a** [G4a]-SHa-treated cell and **b** [G7a]-SHa-treated cell, where $*P<0.05$, $**P<0.01$, and $***P<0.001$ as compared to untreated *S. aureus*

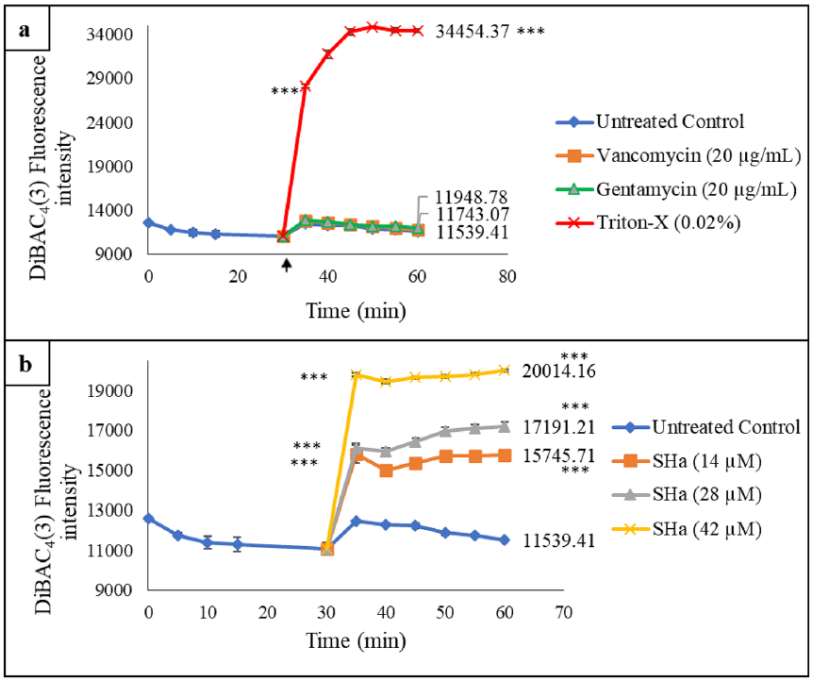

Fig. 6 $DiBAC_4(3)$ uptake kinetic assay of untreated and SHa-treated *S. aureus* (NCTC 13,277). **a** Untreated control and standard drug-treated cells and **b** SHa-treated cell, where $^*P < 0.05$, $^{**}P < 0.01$, and $^{***}P < 0.001$ as compared to untreated *S. aureus*

Biofilm Formation Inhibition Assay

Anti-biofilm activity of peptide analogs was carried out on strong biofilm forming *S. aureus* strain (ATCC 6538). The percentage of biofilm formation inhibition of *S. aureus* (ATCC 6538) after treatment with SHa analogs at different concentrations are shown in Table 6. [G4a]-SHa, [G7a]-SHa, and [G10a]-SHa at concentrations of 6, 12, and 12 µM, respectively, showed more than 90% biofilm formation inhibition. Biofilm images of both untreated and treated *S. aureus* in the 96 well plates are shown in Fig. 8a–g. Bacterial cells treated with 9-µM dose of [G4a]-SHa and [G7a]-SHa and 4 µM of [G10a]-SHa showed small scattered biofilm fragments attached to the periphery of the wells. On the other hand, 8 µM of [G10a]-SHa and 15-µM doses of [G4a]-SHa and [G7a]-SHa completely inhibited the biofilm formation. This shows that [G10a]-SHa possesses a biofilm formation inhibiting capacity at a lower concentration as compared to the other two analogs.

Acute *In Vivo* Toxicity Model

Initially, 25- and 50-mg/kg doses of [G4a]-SHa, [G7a]-SHa, and [G10a]-SHa were dispensed through *i.p.* route to 4 female Balb/c mice/group. All animals were alive for 48 h with no signs of toxicity. Therefore, the dose of all three analogs was increased to 100 mg/kg. Images of vital organs are shown in Fig. 9. At 100-mg/kg dose of [G10a]-SHa, one mouse died in 15–20 min after dosing, while 3 animals remained alive for 48 h but these animals were inactive and weak with black patches seen on their skin. These mice lost an average weight of 0.75 g. Thus, it showed that [G10a]-SHa possesses a toxic effect at 100 mg/kg with 75% survival rate. Unlike [G10a]-SHa, all animals treated with 100 mg/kg, *i.p.* of [G4a]-SHa were healthy and active even after 48 h. Upon dissection, no sign of toxicity was observed on the vital organs. Thus, it showed that [G4a]-SHa has high therapeutic index, and its lethal dose is higher than 100 mg/

Table 6 Percentage biofilm formation inhibition of *S. aureus* (ATCC 6538) after treatment with SHa analogs

Concentration (µM)	% biofilm formation inhibition (mean ± SD)		
	[G10a]-SHa	[G4a]-SHa	[G7a]-SHa
15	> 90	> 90	> 90
12	> 90	> 90	> 90
10	> 90	55 ± 5	65 ± 5
8	> 90	40 ± 3	40 ± 5
6	90 ± 3	15 ± 2	16 ± 4
4	60 ± 5	< 10	< 10
2	20 ± 3	< 5	< 5

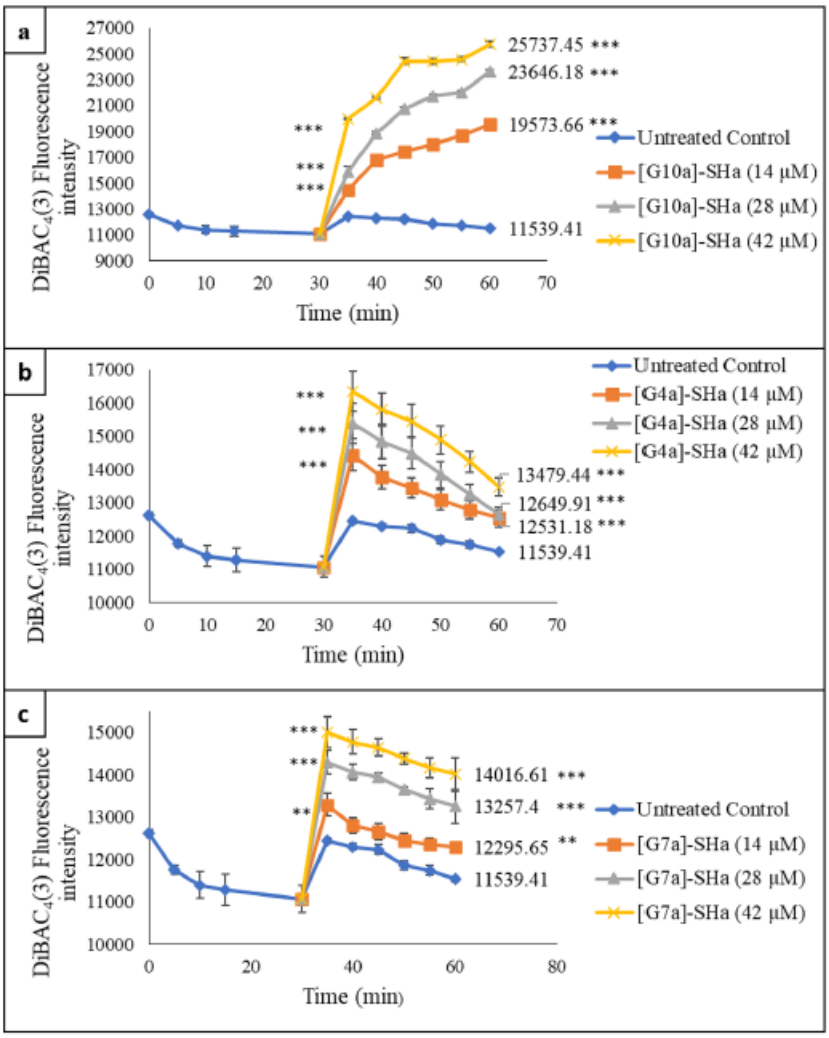

Fig. 7 DiBAC$_4$(3) uptake kinetic assay of *S. aureus* (NCTC 13,277) treated with [G10a]-SHa, [G4a]-SHa, and [G7a]-SHa. **a** [G10a]-SHa-treated cell, **b** [G4a]-SHa-treated cell, and **c** [G7a]-SHa-treated cell, where $*P < 0.05$, $**P < 0.01$, and $***P < 0.001$ as compared to untreated *S. aureus*

kg. In [G7a]-SHa (100 mg/kg, *i.p.*) dosing, all 4 animals were alive for 24 h. After 42 h, one mouse was found to be dead, while the remaining 3 mice were alive for 48 h. It showed 75% survival rate at 100 mg/kg. Upon dissection, stomach of two live and one dead mouse showed signs of diarrhea, while the remaining one alive had normal stomach. As three mice with [G7a]-SHa (100 mg/kg) dosing showed signs of diarrhea; it was given orally (25, 50, and 100 mg/kg) to check its effect on the gastrointestinal system. In oral dosing, all animals were alive and active for 48 h. Upon dissection, no signs of toxicity were found in the stomach, liver, intestine, spleen, and kidney, thus indicating that this analog could be tolerated through oral route. Overall, [G4a]-SHa showed least toxic effect at 100 mg/kg; therefore, the dose could be increased further to find its lethal dose.

Discussion

Among the different AMPs, the temporin family received special attention due to the possibility of generating a new class of peptide-based anti-infective therapeutics [28]. Out of the 120 peptides from temporin family, we selected an anti-bacterial and anti-cancer cationic anti-microbial peptide temporin-SHa as the parent peptide, and synthesized its new peptide analogs in search of analogs that may be better than the parent peptide.

Peptide analogs with D-alanine substitutions in the amino acid sequence at positions 4, 7, and 10 of temporin-SHa were synthesized by solid phase synthesis, and subsequently evaluated for their anti-MRSA activity due to the fact that D-isomers cannot be hydrolyzed by host and bacterial

proteases [29]. These D-alanine substituted analogs demonstrated a good resistivity and stability even at high physiological salt and serum concentrations, thus successfully passing one of the major obstacles in AMP development. Among these analogs, [G10a]-SHa showed the best resistivity and stability at lower concentrations, indicating the importance of 10th position of this peptide for higher serum stability. This serum stability was followed by [G4a]-SHa

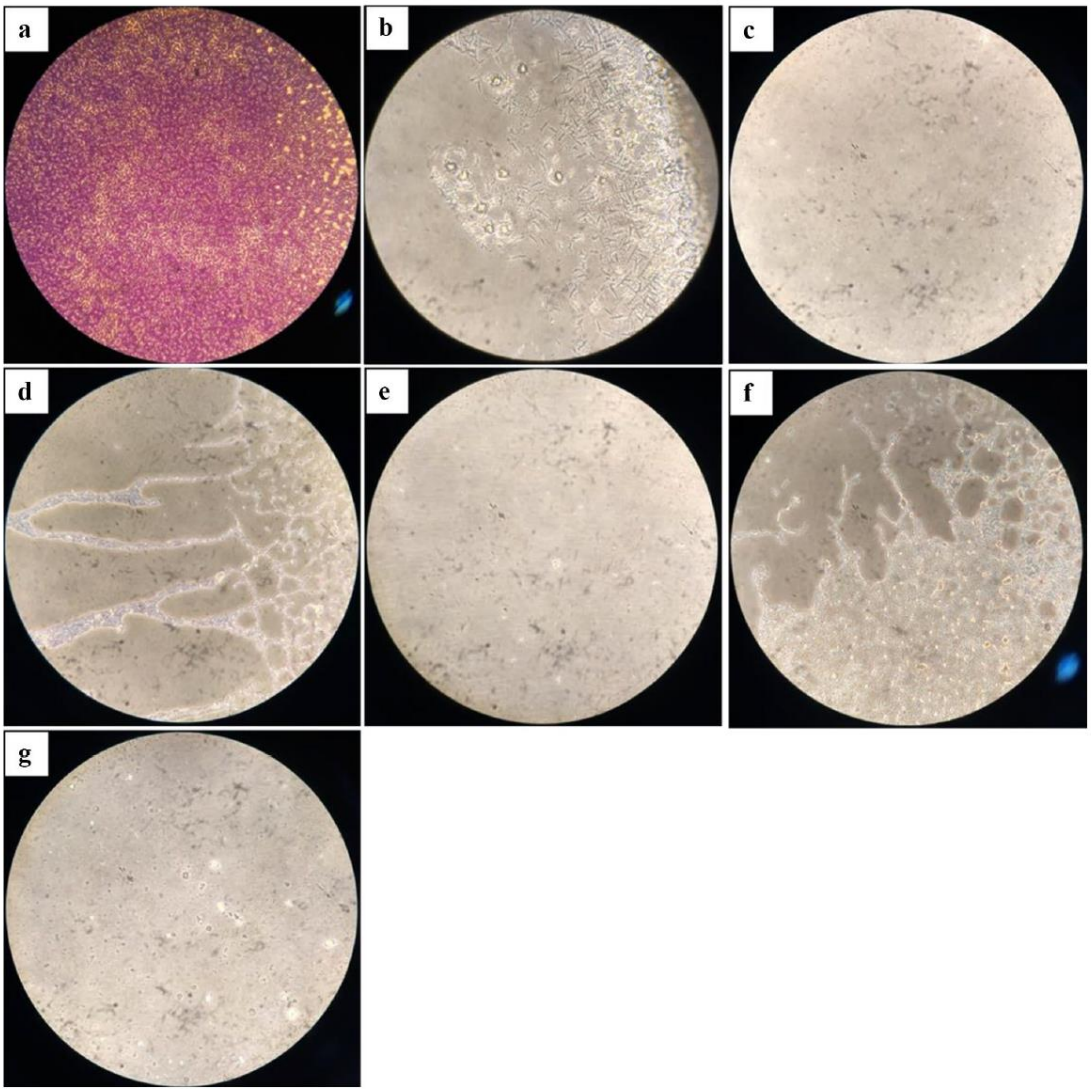

Fig. 8 Biofilm formation of *S. aureus* (ATCC 6538) using crystal violet assay. **a** Untreated control shows full biofilm growth, **b** [G10a]-SHa-treated cells at 4 μM show small amount of remaining biofilm at the periphery of the wells, **c** [G10]-SHa-treated cells at 8 μM show no biofilms, **d** [G4a]-SHa-treated cells at 9 μM shows presence of minor biofilm at the periphery of the wells, **e** [G4a]-SHa-treated cells at 15 μM inhibit the biofilm completely, **f** [G7a]-SHa-treated cells at 9 μM show minor layer of biofilm at the periphery of the wells, and **g** [G7a]-SHa-treated cells at 15 μM demonstrate complete inhibition of biofilm

Fig. 9 Acute *in vivo* toxicity model of SHa analogs at the dose of 100 mg/kg. **a** Untreated control showing no signs of toxicity, **b** and **c** [G10a]-SHa-treated group showing mild black patch on skin indicated by blue arrow, **d** and **e** [G4a]-SHa-treated group showing no toxicity, (**f** and **g**) [G7a]-SHa-treated animals showing discoloration of the stomach indicated by blue arrow, and **h** and **i** [G7a]-SHa-treated animals given oral dose of the peptide demonstrated no signs of toxicity

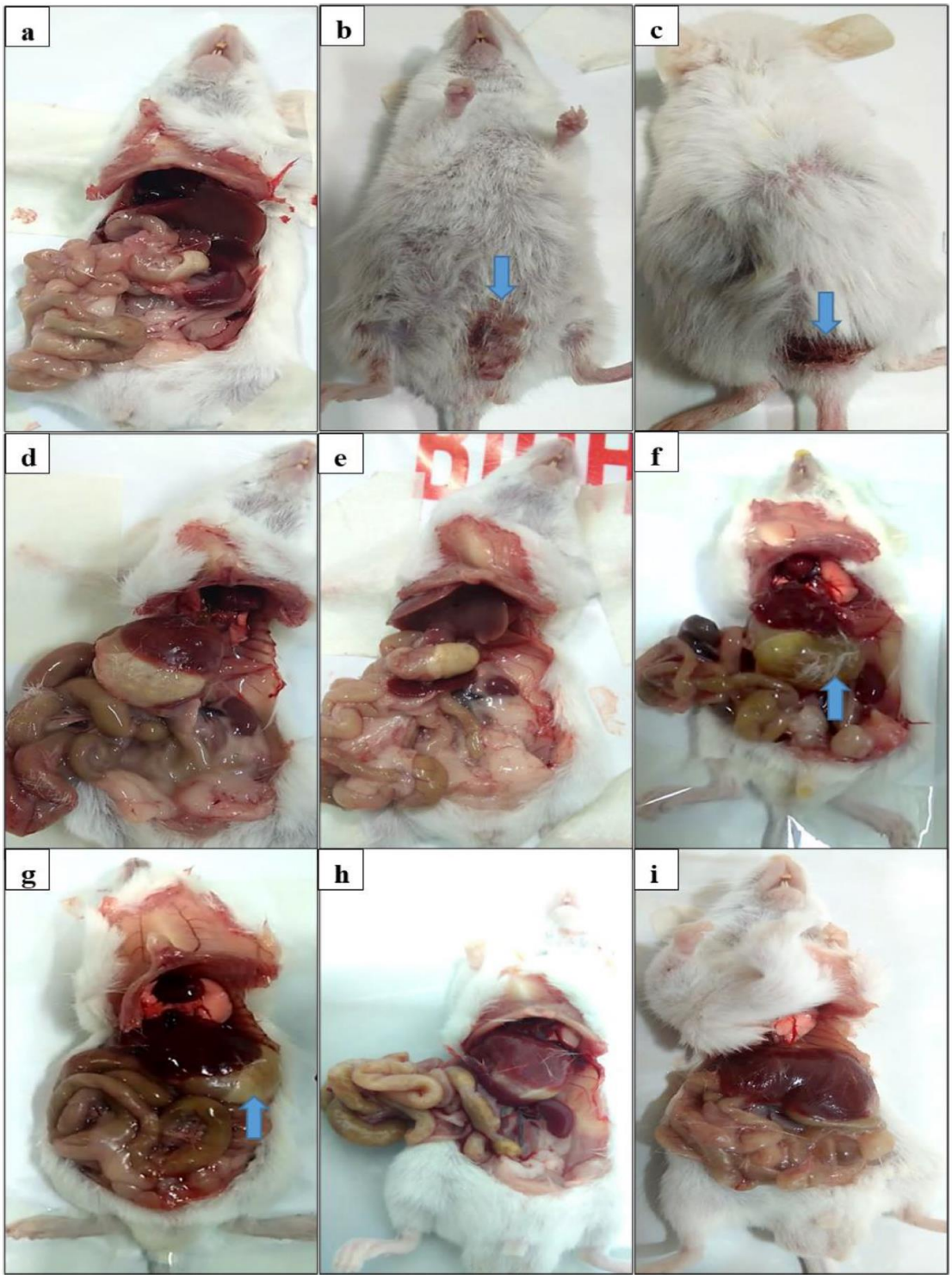
a
b
c
d
e
f
g
h
i

and [G7a]-SHa. This indicated that D-alanine substitution gives serum stability by protecting it from the enzyme proteases present in fetal bovine and human serum.

Therapeutic index (HB_{50}/MIC ratio) and cytotoxicity results showed that [G10a]-SHa was highly hemolytic and cytotoxic just like SHa peptide; hence, it could not be used for systemic application. However, due to its high anti-MRSA activity in lower dose and better stability, it could be tested in *in vivo* skin infection models. Both [G4a]-SHa and [G7a]-SHa were found to be less hemolytic and less cytotoxic to 3T3 cell and Caco2 cell lines at higher concentrations. As [G7a]-SHa showed a high therapeutic index, it was used in acute oral *in vivo* toxicity model. Animals were alive till 100 mg/kg, indicating the non-toxic effect of [G7a]-SHa on gastric lining. Based on [G7a]-SHa oral *in vivo* acute toxicity result, [G4a]-SHa is also predicted to be safe in gastrointestinal tract due to its high therapeutic effect in *in vivo* model, and gastric N87 cell line [16]. *In vivo* acute toxicity study revealed no toxic effects of these analogs up to 50 mg/kg. However, [G10a]-SHa at 100 mg/kg showed a toxic effect; therefore, it is suitable for topical application. Carotenuto et al. proposed "dynamic peptide-lipid supramolecular pore" and "Barrel-Stave" model to interpret the anti-microbial and hemolytic activity of temporin [7]. AFM images of *S. aureus* revealed a rapid effect of these peptides on the cell surface as many cells were seen with ruptured surface along with leakage of cytoplasmic content, demonstrating the membrane rupturing effect of these peptides. Even though, *S. aureus* cells were killed due to treatment with vancomycin and gentamycin, they did not show increase in PI fluorescence as these affected cells still had intact cell membrane, which prevented PI entry inside the dead cells. Vancomycin kills bacteria by inhibiting peptidoglycan cross-bridge formation, and it is reported that it has little effect on cell membrane [30]. Gentamycin crosses the cytoplasmic membrane in response to the internal negative membrane potential of the cell [31] and kills bacteria by inhibiting protein synthesis, because of which cell membrane of the dead cells still show intact cell membrane. Cells treated with these analogs at concentrations $\geq$ MIC showed relatively higher PI fluorescence with increase in incubation time, indicating the increase in cell membrane permeability in a concentration-dependent manner due to loss of membrane integrity. Among the three analogs, [G10a]-SHa showed the highest membrane rupturing ability even at lower concentrations, followed by [G7a]-SHa and [G4a]-SHa.

Clementi et al. [25], by using $DiBAC_4(3)$ and PI dye, simultaneously showed that $DiBAC_4(3)$ fluorescence increased ahead of increase in PI fluorescence, indicating that membrane potential depolarization occurred prior to cell membrane rupture. Vancomycin and gentamycin did not show increase in $DiBAC_4(3)$ fluorescence, indicating their non-significant effect on the cell membrane [30]. SHa and [G10a]-SHa caused membrane depolarization in a concentration-dependent manner, and increased with incubation time. As SHa and [G10a]-SHa exhibited a high membrane depolarizing activity and this may be the reason behind their hemolytic activity, as this property enhances the membrane permeability.

[G10a]-SHa inhibited biofilm formation of *S. aureus* (ATCC 6538) at a lower concentration. Therefore, to confirm its mature biofilm disrupting effect, our next target will be to study further its mature biofilm eradication property, and its possible use as anti-adhesive coating on different surfaces.

Conclusion

D-alanine substituted analogs of temporin-SHa showed high serum and salt-resistant potential. [G4a]-SHa and [G7a]-SHa triggered rapid anti-MRSA activity, primarily through membrane disruption, with less toxic effect towards mammalian cells. Highly potent [G10a]-SHa, due to its hemolytic activity, might be suitable for topical applications, whereas [G4a]-SHa and [G7a]-SHa would be explored for their possible systemic application. Therefore, further in vivo findings are needed to evaluate their chronic toxicity, immunogenic activity, and therapeutic profile.

Funding This study was supported by the Higher Education Commission, Project NRPU 5738 and 8169/Sindh/NRPU/R&D/HEC.

Data Availability All data generated or analyzed during this study are included in this submitted article and also available from the corresponding author on reasonable request.

Declarations

Conflict of Interest The authors declare no competing interests.

References

1. Ventola CL (2015) The antibiotic resistance crisis: part 1: causes and threats. P T 40(4):277–283
2. Hiramatsu K, Aritaka N, Hanaki H et al (1997) Dissemination in Japanese hospitals of strains of *Staphylococcus aureus* heterogeneously resistant to vancomycin. Lancet 350:1670–1673. https://doi.org/10.1016/S0140-6736(97)07324-8
3. Conlon JM, Kolodziejek J, Nowotny N (2004) Antimicrobial peptides from ranid frogs: taxonomic and phylogenetic markers and a potential source of new therapeutic agents. Biochim Biophys Acta 1696:1–14. https://doi.org/10.1016/j.bbapap.2003.09.004
4. Simmaco M, Mignogna G, Canofeni S et al (1996) Temporins, antimicrobial peptides from the European red frog *Rana temporaria*. Eur J Biochem 242:788–792. https://doi.org/10.1111/j.1432-1033.1996.0788r.x
5. Seo MD, Won HS, Kim JH et al (2012) Antimicrobial peptides for therapeutic applications: a review. Molecules 17:12276–12286. https://doi.org/10.3390/molecules171012276

6. Abbassi F, Galanth C, Amiche M et al (2008) Solution structure and model membrane interactions of temporins-SHa, antimicrobial peptides from amphibian skin. A NMR spectroscopy and differential scanning calorimetry study. Biochemistry 47:10513–10525. https://doi.org/10.1021/bi8006884
7. Carotenuto A, Malfi S, Saviello MR et al (2008) A different molecular mechanism underlying antimicrobial and hemolytic actions of temporins A and L. J Med Chem 51:2354–2362. https://doi.org/10.1021/jm701604t
8. Mangoni ML, Shai Y (2011) Short native antimicrobial peptides and engineered ultrashort lipopeptides: similarities and differences in cell specificities and modes of action. Cell Mol Life Sci 68:2267. https://doi.org/10.1007/s00018-011-0718-2
9. Mangoni ML, Shai Y (2009) Temporins and their synergism against Gram-negative bacteria and in lipopolysaccharide detoxification. Biochim Biophys Acta 1788:1610–1619. https://doi.org/10.1016/j.bbamem.2009.04.021
10. Mahalka AK, Kinnunen PKJ (2009) Binding of amphipathic α-helical antimicrobial peptides to lipid membranes: lessons from temporins B and L. Biochim Biophys Acta 1788:1600–1609. https://doi.org/10.1016/j.bbamem.2009.04.012
11. Abbassi F, Oury B, Blasco T et al (2008) Isolation, characterization and molecular cloning of new temporins from the skin of the North African ranid Pelophylax saharica. Peptides 29:1526–1533. https://doi.org/10.1016/j.peptides.2008.05.008
12. Ladram A, Sereno D, Abbassi F et al (2010) Analogs of temporin-SHa, and uses thereof. U.S. Patent No. 9,522,942. Washington, DC: U.S. Patent and Trademark Office
13. Raja Z, Andre S, Abbassi F et al (2017) Insight into the mechanism of action of temporin-SHa, a new broad-spectrum antiparasitic and antibacterial agent. PLoS One 12:e0174024. https://doi.org/10.1371/journal.pone.0174024
14. Lombana A, Raja Z, Casale S et al (2014) Temporin-SHa peptides grafted on gold surfaces display antibacterial activity. J Pept Sci 20:563–569. https://doi.org/10.1002/psc.2654
15. Oger PC, Piesse C, Ladram A et al (2019) Engineering of antimicrobial surfaces by using temporin analogs to tune the biocidal/antiadhesive effect. Molecules 24:814. https://doi.org/10.3390/molecules24040814
16. OlleikH BE, Perrier J et al (2019) Temporin-SHa and its analogs as potential candidates for the treatment of *Helicobacter pylori*. Biomolecules 9:598. https://doi.org/10.3390/biom9100598
17. Crépin A, Jegou JF, Andre S et al (2020) *In vitro* and intracellular activities of frog skin temporins against *Legionella pneumophila* and its eukaryotic hosts. Sci Rep 10:1–14. https://doi.org/10.1038/s41598-020-60829-2
18. Shaheen F, Haque MN, Ahmed A et al (2018) Synthesis of breast cancer targeting conjugate of temporin-SHa analog and its effect on pro-and anti-apoptotic protein expression in MCF-7 cells. Peptides 106:68–82. https://doi.org/10.1016/j.peptides.2018.07.002
19. Shah ZA, Farooq S, Ali SA et al (2018) New analogs of temporin-LK1 as inhibitors of multidrug-resistant (MDR) bacterial pathogens. Synth Commun 48:1172–1182. https://doi.org/10.1080/00397911.2018.1437450
20. Wikler MA (2006) Methods for dilution antimicrobial susceptibility tests for bacteria that grow aerobically: approved standard. CLSI (NCCLS) 26:M7-A7
21. Lancaster MV, Fields RD (1996) Antibiotic and cytotoxic drug susceptibility assays using resazurin and poising agents. U.S. Patent 5,501,959. Washington, DC: U.S. Patent and Trademark Office
22. Wiradharma N, Khoe U, Hauser CAE et al (2011) Synthetic cationic amphiphilic α-helical peptides as antimicrobial agents. Biomaterials 32:2204–2212. https://doi.org/10.1016/j.biomaterials.2010.11.054
23. Tolosa L, Donato MT, Lechon MJG et al (2015) General cytotoxicity assessment by means of the MTT assay, in Protocols in *In Vitro* Hepatocyte Research Springer. 333–348. https://doi.org/10.1007/978-1-4939-2074-7_26
24. Meincken M, Holroyd DL, Rautenbach M (2005) Atomic force microscopy study of the effect of antimicrobial peptides on the cell envelope of *Escherichia coli*. Antimicrob Agents Chemother 49(10):4085–4092. https://doi.org/10.1128/AAC.49.10.4085-4092.2005
25. Clementi EA, Marks LR, Hakansson HR et al (2014) Monitoring changes in membrane polarity, membrane integrity, and intracellular ion concentrations in *Streptococcus pneumoniae* using fluorescent dyes. J Vis Ex 84:e51008. https://doi.org/10.3791/51008
26. Arshia KAK, Khan KM et al (2017) Antibiofilm potential of synthetic 2-amino-5-chlorobenzophenone Schiff bases and its confirmation through fluorescence microscopy. Microb Pathog 110:497–506. https://doi.org/10.1016/j.micpath.2017.07.040
27. Botham PA (2004) Acute systemic toxicity—prospects for tiered testing strategies. Toxicol *In Vitro* 18:227–230. https://doi.org/10.1016/s0887-2333(03)00143-7
28. Mangoni ML, M., Grazia A D, Cappiello F, et al (2016) Naturally occurring peptides from *Rana temporaria*: antimicrobial properties and more. Curr Top Med Chem 16:54–64. https://doi.org/10.2174/1568026615666150703121403
29. Qiu S, Zhu R, Zhao Y et al (2017) Antimicrobial activity and stability of protonectin with D-amino acid substitutions. J Pept Sci 23(5):392–402. https://doi.org/10.1002/psc.2989
30. Huang E, Yousef AE (2014) The lipopeptide antibiotic paenibacterin binds to the bacterial outer membrane and exerts bactericidal activity through cytoplasmic membrane damage. Appl Environ Microbiol 80:2700–2704. https://doi.org/10.1128/AEM.03775-13
31. Damper PD, Epstein W (1981) Role of the membrane potential in bacterial resistance to aminoglycoside antibiotics. Antimicrob Agents Chemother 20(6):803–808. https://doi.org/10.1128/aac.20.6.803